

Inertial Coupling of Resonant Normal Modes in Rotating Cavities: Acoustic Gyrometers for High Rotation Rates

David Ecotière, Najat Tahani, Michel Bruneau

Laboratoire d'Acoustique de l'Université du Maine, UMR CNRS 6613, Université du Maine, Av. O. Messiaen, 72 085 Le Mans cedex, France. michel.bruneau@univ-lemans.fr

Summary

For steady rotations, acoustic rate gyros involve inertial coupling between acoustic modes inside rotating cylindrical fluid-filled resonant cavities. Previous studies investigated acoustic rate gyros of small dimensions (using silicon technology) and high dynamic range for measurement of transient or stationary rotation rates (from $0.01^\circ/\text{s}$ up to $1000^\circ/\text{s}$), which can be applied to a wide variety of applications. Herein investigated are very high rotation rates (up to $10^5^\circ/\text{s}$) and the phenomena they cause, namely the effects of the non uniformity of the fluid on the acoustic field inside the rotating cavity and the effects of the recurrent inertial coupling between the preponderant acoustic modes. Results of measurements confirm the analytical predictions and requirements for designing rapidly spinning gyrometers behaving linearly are discussed.

PACS no. 43.20.Ks, 43.35.Ty, 42.81.Pa

1. Introduction

An acoustic rate gyro provides output signals that are measures of angular rates with respect to an inertial frame. It involves both inertial coupling between acoustic modes inside rotating cylindrical fluid-filled resonant cavities and flow-induced acoustic modes coupling, the former occurring for transient and stationary rotation of the device, the later occurring only for the transient rotation. The physical phenomena, namely the characteristics of unsteady circular flow which occurs when the cylindrical cavity is set in rotation around its axis, the shape and the stabilisation time of the transient response (i.e. the output acoustic signal giving measure of the rotation rate), the linear relationship between this output acoustic signal and rotation rate, were interpreted for rotation rates from $0.01^\circ/\text{s}$ (the threshold of the small gyros, about 1 cm^3) up to $1000^\circ/\text{s}$ (that is 10^5 times the threshold). Excellent agreements were observed between the theoretical and experimental results [1, 2, 3, 4].

These investigations provide a method for designing this new kind of acoustic sensor (rate gyro) involving lower power consumption and lower manufacturing cost, as well as improved reliability and improved live time. Moreover, recent studies using silicon technology [5, 6, 7] pointed out that the acoustic gyro (fluid-filled cavity with a loudspeaker and two microphones set on the walls) can be extremely miniaturised to meet growing industrial re-

quirements. Research on the acoustic gyro is now focusing on developing a technology to measure very high rotation rates (up to $10^5^\circ/\text{s}$). Then, the aim of this paper is both – i) to investigate the behavior of the acoustic gyro for these very high angular velocities that give rise to new phenomena (namely the effects of the non uniform properties of the fluid on the acoustic field, and the recurrent inertial coupling between the preponderant acoustic modes), and – ii) to show that the acoustic gyro is suitable for applications where very high rotation rates occur.

To understand the acoustic coupling mechanisms for higher rotation rates, the model presented below starts with the theory for unsteady rotation [4]. To adapt this theory to the purpose, we neglect the specific factors which occur for very fast variations of the rotation rate of the cavity, but we do not longer assume both the uniformity of the density of the fluid (as a consequence of the centripetal acceleration) and Born approximation (usually assumed when the inertial effects, which depend on the acoustic field created by the loudspeaker, can be considered as very small perturbations).

Sections 2.1 and 2.2 review respectively the mechanisms inherent to the acoustic gyrometer and the basic equations of motion, including specific factors that occur at high rotation rates. Section 3.1 presents the modeling of the phenomena involved and the analytical results for an angular velocity lying from $0^\circ/\text{s}$ to $10^5^\circ/\text{s}$, and the last section (3.2) compares the theoretical and experimental results (showing that the model is valid) and conclude on the design of the devices for measuring very high rotation rates.

Received 30 June 2003,
accepted 6 May 2004.

2. Formulation of the problem

2.1. The mechanisms involved

The heart of the acoustic gyro is the thin cylindrical cavity filled with gas sketched in Figure 1, thin meaning that the height h is much lower than the radius R to ensure a quasi uniform field through the cavity along the z -axis. An harmonic acoustic standing wave is generated by a driver coupled to the cavity through a narrow hole set at the azimuthal coordinate $\varphi = 0$. In order to increase the acoustic level and then the sensitivity of the gyrometer the angular frequency is the resonant frequency of the first azimuthal mode labeled “ c ” and given by the eigenfunction $J_1(\gamma_{10}r/R) \cos \varphi$ corresponding to the values $(0,1,0)$ of the quantum numbers (n_r, n_φ, n_z) respectively, where J_1 is the first order cylindrical Bessel function of the first kind, γ_{10} the first zero of the first derivative of $J_1(\gamma_{10}r/R)$ with respect to the radial coordinate r . A microphone set at $\varphi = \pi/2$ (flush-mounted or coupled to the cavity through a hole) measures the amplitude of the acoustic field, which vanishes at that point when the cavity does not rotates.

When the cylindrical cavity rotates around its z -axis, that is when the fluid rotates with the angular velocities $\vec{\Omega}(r, z, t)$ of the non inertial frames (linked to the particles of fluid) with respect to the inertial frame, two kinds of effects must be considered, namely the dependence of the field created by the loudspeaker on the non-uniform properties of the rotating fluid and the inertial effects on the acoustic field. The non uniform properties of the fluid involve both the angular particle velocities (when they depend on both the localization of the particle in the cavity and the time) and the non uniformity of the density of the fluid due to the centripetal acceleration (especially at higher rotation rates). The inertial effects on the acoustic field are the three well known ones, that is the Coriolis effect, the effect of the acceleration associated with the time rate of change of the rotational velocity, and the centripetal acceleration effect. In these conditions, the field created by the loudspeaker is perturbed, leading to energy transfer from the resonant mode labeled “ c ” mentioned above to the orthogonal resonant mode labeled “ s ” given by the eigenfunction $J_1(\gamma_{10}r/R) \sin \varphi$. Then the transfer function between the output signal of the microphone set at $\varphi = \pi/2$ (which measures the amplitude of the mode “ s ”) and the output signal of another microphone set at $\varphi = \pi$ (which measures the amplitude of the mode “ c ”), provides the value of the rotation rate of the cavity. These two resonant modes “ c ” and “ s ” are almost sufficient to describe a solution for the acoustic response of the rotating cavity, in the “ideal” case of a perfectly shaped cavity ; actually, in order to take into account unavoidable small perturbations, more terms can be included into the eigenfunctions expansion which is used to describe the acoustic field [2].

It is noteworthy that the inertial forces can be interpreted [1, 2, 3, 4] in the acoustic wave equation as a source term given by $\vec{\nabla} \cdot \vec{f}$, that is for the Coriolis force \vec{f}_c (for example)

$$\vec{\nabla} \cdot \vec{f}_c = \rho_0 \vec{\nabla} \cdot (2\vec{\Omega} \times \vec{v}) = \rho_0 2\vec{\Omega} \cdot (\vec{\nabla} \times \vec{v}), \quad (1)$$

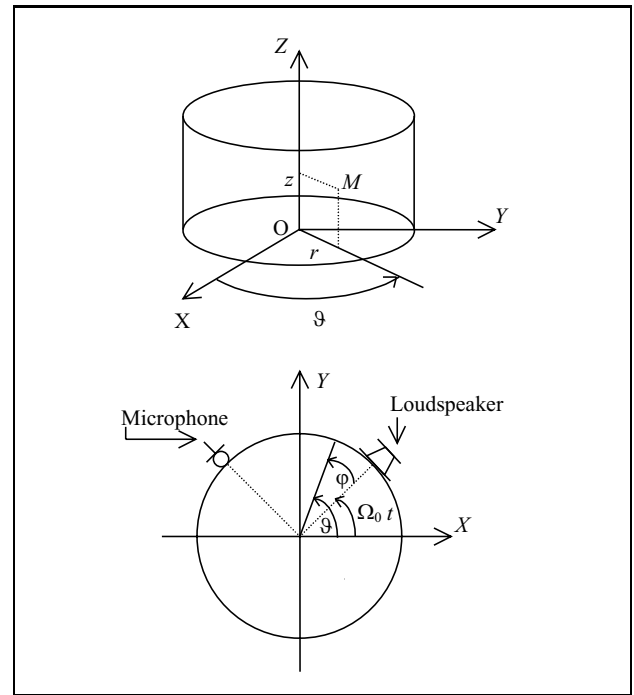


Figure 1. Acoustic rate gyro: cylindrical fluid-filled cavity. The cavity (lateral view and top view), localisation of the transducers, inertial (O, X, Y, Z) and non inertial (M, r, φ, z) reference frames.

(where ρ_0 is the density of the gas) emphasizing that the vortical component \vec{v}_v of the particle velocity \vec{v} ($\vec{\nabla} \times \vec{v} = \vec{\nabla} \times \vec{v}_v$) plays an important role in the inertial coupling. This vortical component is almost negligible everywhere except inside the viscous boundary layers, which therefore play an important role in the process, especially in shortening drastically the stabilization time of the acoustic transient response in comparison with the stabilization time of the transient rotating flow [4] (when the gyro is suddenly set in rotation for example). Moreover, because resonant modes are involved (to improve the sensitivity of the rate gyros), the dissipation processes due to viscous and thermal phenomena, which occur essentially inside the boundary layers, must be taken into account.

2.2. The basic equations of motion

In the acoustic gyro, the whole motion of the fluid (represented by the particle velocity \vec{V}_T) includes the circular flow ($\vec{V}(r) = \vec{\Omega} \times \vec{r}$) and an “acoustic” motion (velocity \vec{v}), the word “acoustic” being taken here globally because it includes the thermal (\vec{v}_h) and vortical (\vec{v}_v) motions which accompany the acoustic movement itself (\vec{v}_a). Describing the instantaneous position of a particle by means of the vector \vec{OP} , the particle velocity and the acceleration associated to the global motion are written respectively as

$$\vec{V}_T = d_t)_i \vec{OP} \quad \text{and} \quad d_t)_i \vec{V}_T = d_{tt}^2)_i \vec{OP}, \quad (2)$$

where the operator $d_t)_i$ is the material derivative expressed in an inertial reference frame, and considering the “acous-

tic” movement only, its acceleration is given by the material derivative $d_t \vec{v}$.

Considering here the stationary regime, the cylindrical cavity and the fluid rotating together with a uniform angular velocity Ω , the fluid and the transducers (the localized acoustic source and the microphone) remain continuously motionless each one with regard to the others and, within the framework of the linear acoustics, the material derivative with respect to the time in the moving frame is equal to the partial derivative ∂_t in the same frame.

Then the “acoustic” particle acceleration expressed in the inertial reference frame takes the approximate form

$$\partial_t \vec{v} + 2\vec{\Omega} \times \vec{v} + 2\vec{\Omega} \times (\vec{\Omega} \times \partial_t^{-1} \vec{v}), \tag{3}$$

where $\partial_t^{-1} \vec{v}$ represents the “acoustic” particle displacement, the inertial factor $\partial_t \vec{\Omega} \times \partial_t^{-1} \vec{v}$ vanishing because $\partial_t \vec{\Omega}$ is assumed here to be equal to zero.

Moreover, when strong rotation rates occur, the effects of the centripetal acceleration on the static pressure P_0 , given by

$$\partial_r P_0 = \rho_0 r \Omega^2, \tag{4}$$

induce a radial density variation which takes the form, for a perfect gas,

$$\partial_r \rho_0 = \frac{\rho_0}{p_0} \partial_r P_0 = \chi_T \rho_0^2 r \Omega^2, \tag{5}$$

where χ_T is the isothermal compressibility, this radial density variation taking into account the inertial non uniformity of the medium where the acoustic field propagates.

Finally, the “acoustic” movement (that is the sum of the acoustic, entropic and vortical movements) is governed by a set of three equations including the Stokes-Navier equation, the conservation of mass equation and the heat equation, namely (the acoustic energy source being described by its volume velocity q):

$$\begin{aligned} \partial_t \vec{v} + 2\vec{\Omega} \times \vec{v} + \vec{\Omega} \times (\vec{\Omega} \times \partial_t^{-1} \vec{v}) + \frac{1}{\rho_0 \vec{\nabla} p} \\ = \nu \Delta \vec{v} + \left(\frac{\eta}{\rho_0} + \frac{\nu}{3} \right) \vec{\nabla} \vec{\nabla} \cdot \vec{v}, \end{aligned} \tag{6}$$

where ν is the kinematic viscosity coefficient, η the bulk viscosity coefficient, and p the pressure variation,

$$\partial_t \rho' + \rho_0 \vec{\nabla} \cdot \vec{v} = \rho_0 q, \tag{7}$$

where ρ' is the density variation,

$$\partial_t \tau - \frac{\lambda}{\rho_0 C_p} \Delta \tau = \frac{\gamma - 1}{\beta \gamma} \partial_t p, \tag{8}$$

where τ is the temperature variation, λ the thermal conductivity coefficient, C_p the heat coefficient at constant pressure per unit of mass and β the increase in pressure per unit increase in temperature at constant density.

When the time-periodic source activity of the localized loudspeaker set on the cylindrical wall is given by the real

part of the harmonic rate of creation of fluid per unit volume

$$q = Q e^{i\omega t} = Q_0 \frac{\delta(r - R)}{r} \delta(\varphi) e^{i\omega t}, \tag{9}$$

the solutions of equations (6) to (8), invoking expression (5) for the stationary density variation and the usual relationship $c_0^2 \rho' = p - \beta \tau$ for the “acoustic” density (where c_0 is the adiabatic speed of sound), and subject to the boundary conditions (on the walls $z = 0, z = h$ or $r = R$) for the temperature variation and the “acoustic” particle velocity, namely

$$\tau = 0 \quad \text{and} \quad \vec{v} = \vec{0}, \tag{10}$$

are the appropriate results that are needed to interpret the experimental data available (section 3.2).

The inertial factors (equation 6) involve the expression of the whole “acoustic” particle velocity (equation 1), the sum of the laminar acoustic and laminar thermal velocities \vec{v}_a and \vec{v}_h , and the vortical velocity \vec{v}_v (which plays an important role in the inertial coupling). The thermal and vortical velocities are negligible in comparison with the laminar acoustic velocity in the whole domain under consideration (the volume of the cavity) except in the boundary layers near the walls (because on the walls the particle velocity and the temperature variation vanish). Accurate description of the small amplitude disturbances, based on a set of equations derived from equations (6) to (10), independently of the inertial effects, gives a relationship between the r - and φ -components of the particle velocity \vec{v} and the pressure variation p as follows, for an harmonic motion at an angular frequency ω close to the eigen angular frequency ω_{10} (see e.g. [4, 8, 9]):

$$\begin{aligned} v_r \approx \frac{i}{\rho_0 c_0} (1 - F_v) \left[\frac{1}{k} \partial_r p + \left(\frac{1}{\gamma_{10}^2} \frac{k}{ik_v} \left(1 - e^{-ik_v(R-r)} \right) \right. \right. \\ \left. \left. + (\gamma - 1) \frac{k}{ik_h} \left(1 - e^{-ik_h(R-r)} \right) \right) p \right], \end{aligned} \tag{11}$$

$$v_\varphi \approx \frac{i}{\rho_0 c_0} (1 - F_v) \left[\frac{1}{kr} \left(1 - e^{-ik_v(R-r)} \right) \partial_\varphi p \right], \tag{12}$$

where $F_v = e^{-ik_v z} + e^{-ik_v(h-z)},$
 $k_v = \frac{(1-i)}{\delta_v}, \quad k_h = \frac{(1-i)}{\delta_h},$ \tag{13}

with $\delta_v = \sqrt{2\nu/\omega}$ and $\delta_h = \sqrt{2\lambda/\rho_0 C_p \omega}$ (viscous and thermal boundary layer thicknesses), $\gamma_{10} = k_{10} R = \omega_{10} R / c_0$ being the eigenvalue of the eigenmodes considered. Because the height h of the cavity is greater than the viscous boundary layer thickness, the function $(1 - F_v)$ vanishes on the walls $z = 0$ and $z = h$, which therefore are not directly involved in the inertial modes coupling.

It is noteworthy that the vortical (\vec{v}_v) and thermal (\vec{v}_h) velocities are given by the factors involving $e^{-ik_v(R-r)}$ and $e^{-ik_h(R-r)}$ respectively. The sum of the other factors represents the acoustic velocity in the thermo-viscous fluid, emphasizing the well known impedance like behavior of the acoustic field near the boundaries which can be

expressed as a specific admittance $\beta = \rho_0 c_0 v_{ar} / p$ (the pressure variation being assumed to be constant over the boundary layer thicknesses) given here by

$$\beta = k \left(\frac{1/\gamma_{10}^2}{k_v} + \frac{\gamma - 1}{k_h} \right). \quad (14)$$

At this step, we must proceed with the derivation of the relevant solution of the set of equations which govern the acoustic pressure field p inside the rotating cavity (equations 5 to 10). Due the fact that the working frequency is monitored to make this field resonant (namely the frequency is tuned on the resonant frequency of the first azimuthal modes of the cavity), the viscous and thermal dissipations must be taken into account. Actually they are included in this set of equations, but inspection of them with consideration of the orders of magnitude of the quantities involved reveals that the dissipation occurs mainly inside the viscous and thermal boundary layers (the dissipation processes in the bulk of the cavity being then negligible), which therefore can be modeled by a boundary condition involving the equivalent impedance β mentioned above (equation 14). Then discarding terms which depend on viscosity and thermal conduction in the right hand side of equations of motion (6) and (8), and taking account equation (5) to express the effect of the inertial non uniformity of the density $\vec{\nabla}(1/\rho_0) \cdot \vec{\nabla}(p) = \partial_r(1/\rho_0)\partial_r p$, the pressure variation (assumed to be quasi-independent of the coordinate z) is governed by the following set of equations, for the angular frequency ω close to the eigen one ω_{10} (the factor $e^{i\omega t}$ being omitted):

$$\left[\partial_{rr}^2 + \frac{1}{r} \partial_r + \frac{1}{r^2} \partial_{\varphi\varphi} + k^2 \right] p = - \left[S + F_{Co} + F_{Ce} + F_{nh} \right] \quad (15)$$

in the bulk of the cavity,

$$(\partial_n + ik\beta)p = 0 \quad (16)$$

on the boundaries $r = R$ and $z = 0$ or h , where

$$S = i\omega \rho_0 Q_0 \frac{\delta(r - R)}{r} \delta(\varphi) \quad (17)$$

is the source term,

$$F_{Co} = \rho_0 \operatorname{div}(2\vec{\Omega} \times \vec{v}) = -2\rho_0 \Omega_0 (\overrightarrow{\operatorname{curl}} \vec{v})_z \\ = -2\rho_0 \Omega_0 \left[\left(\frac{1}{r} + \partial_r \right) v_\varphi - \frac{1}{r} + \partial_\varphi \right) v_r \right] \quad (18)$$

is the Coriolis factor,

$$F_{Ce} = \rho_0 \operatorname{div}[\vec{\Omega} \times (\vec{\Omega} \times \vec{v}/i\omega)] \\ = -\frac{\rho_0}{i\omega} \left[\left(\frac{1}{r} + \partial_r \right) v_r + \frac{1}{r} + \partial_\varphi v_\varphi \right] \Omega_0^2 \quad (19)$$

is the centripetal factor,

$$F_{nh} = -\frac{\gamma \Omega_0^2}{c_0^2} r \partial_r p \quad (20)$$

is the non homogeneity factor due to the centripetal effect on the fluid density, the r - and φ -components of the particle velocity being given by their expressions (11) and (12) as functions of the pressure variation p (assuming $(1 - F_V) \approx 1$) and the admittance β being given by equation (14).

Associating to this problem the Green function solution of equation

$$\left[\partial_{rr}^2 + \frac{1}{r} \partial_r + \frac{1}{r^2} \partial_{\varphi\varphi} + k^2 \right] G(\vec{r}, \vec{r}_0) \\ = -\frac{\delta(r - r_0)}{r} \delta(\varphi - \varphi_0), \quad (21)$$

which satisfies the same boundary condition (16) than the pressure variation p , namely $(\partial_r + ik\beta)G = 0$, the “solution” of the set of equations (15) to (20) can be written as the convolution, with respect to the variables (r, φ) , of the right hand side of equation (15) and the Green function:

$$p = h \int_0^R \int_0^{2\pi} r dr d\varphi \left(G[S + F_{Co} + F_{Ce} + F_{nh}] \right). \quad (22a)$$

For compactness, in the following this equation is written using the Dirac notation, namely

$$p = \left\langle G \left| S + F_{Co} + F_{Ce} + F_{nh} \right. \right\rangle. \quad (22b)$$

Because the analysis of the cavity excitation relies on modal functions of the domain, labeled $(0,1,0)$ “c” or “s”, together with their related eigenvalues ω_{10} , for the angular frequency of interest monitored at (or close to) the resonance of these modes, the Green function chosen is expressed as an eigenfunction expansion restricted to these two resonant modes of the cavity, namely [8, 9, 4]

$$G(\vec{r}, \vec{r}_0) \approx \frac{\psi_c(\vec{r})\psi_c(\vec{r}_0) + \psi_s(\vec{r})\psi_s(\vec{r}_0)}{k_{10}^2 + (i-1)\chi_1^2 - k^2}, \quad (23)$$

where the eigenfunctions $\psi_{c,s}$ can be considered as a zero order expansion with respect to β , i. e.

$$\psi_c(\vec{r}, \varphi) \approx N^{-1} J_1(k_{10}r) \cos \varphi, \\ \psi_s(\vec{r}, \varphi) \approx N^{-1} J_1(k_{10}r) \sin \varphi,$$

with $N = J_1(\gamma_{10} \sqrt{1 - 1/\gamma_{10}^2} \sqrt{\pi R^2 h/2})$, $k_{10} = \gamma_{10} = 1.84$, and where the weighted boundary dissipation factor χ_1^2 is given by

$$\chi_1^2 \approx k_{10} \iint_S \frac{\beta}{1+i} \psi_{c,s}^2 dS \\ = k_{10}^2 \left[\frac{1}{h} (\delta_v + (\gamma-1)\delta_h) \right. \\ \left. + \frac{\gamma_{10}^2}{R(\gamma_{10}^2 - 1)} \left(\frac{1}{\gamma_{10}^2} \delta_v + (\gamma-1)\delta_h \right) \right].$$

Expression (22) for the solution p is in fact an integral equation because the functions F_{Co} , F_{Ce} , and F_{nh} depend on the unknown function p . The appropriate solution, that is eigenfunction expansion used in the next section,

$$p = A_c \psi_c(\vec{r}) + A_s \psi_s(\vec{r}), \quad (24)$$

will give both the amplitude A_c , measured by the microphone set at $\varphi = 0$ (in practice set opposite to the source at $\varphi = \pi$), and the amplitude A_s , measured by the microphone set at $\varphi = \pi/2$, and finally the transfer function A_s/A_c which gives measure of the rotation rate Ω .

3. The inertial effects

3.1. Modal theory of the inertial coupling

Expressing the pressure variation p as a truncated eigenfunction expansion (24) in the expression (11) and (12) of the r - and φ -components of the particle velocity, and then in expression (18), (19), and (20) for the inertial factors F_{Co} , F_{Ce} , and F_{nh} , assuming that the angular frequency ω remains close to the eigen angular frequency ω_{10} , and taking into account the orthogonality properties of the eigenfunctions ψ_s and ψ_c , each factor appearing in equation (22b) can be expressed straightforwardly in the following manner:

$$\langle G|S \rangle = \frac{S}{D} \psi_c, \tag{25}$$

$$\begin{aligned} \langle G|F_{Co} \rangle &= \langle G|f_{Co} \partial_\varphi |p \rangle \\ &= \frac{\psi_c}{D} \langle \psi_c | f_{Co} - A_s \psi_c \rangle \\ &\quad + \frac{\psi_s}{D} \langle \psi_s | f_{Co} A_c \psi_c \rangle \\ &= \frac{C_o}{D} (A_s \psi_c + A_c \psi_s), \end{aligned} \tag{26}$$

$$\begin{aligned} \langle G|F_{Ce} + F_{nh} \rangle &= \frac{\psi_c}{D} \langle \psi_c | f_{Ce} + f_{nh} |p \rangle \\ &= \frac{\psi_c}{D} \langle \psi_c | f_{Ce} + f_{nh} |A_c \psi_c \rangle \\ &\quad + \frac{\psi_s}{D} \langle \psi_s | f_{Ce} + f_{nh} |A_s \psi_s \rangle \\ &= \frac{C_e}{D} (A_c \psi_c + A_s \psi_s), \end{aligned} \tag{27}$$

where f_{Co} , f_{Ce} , and f_{nh} are operators which do not contain odd derivatives with respect to the variable φ (these operators do not change $\cos \varphi$ into $\sin \varphi$ and inversely) and which do not depend on φ , and where

$$D = k_{10}^2 + (i + 1)\chi_1^2 - k^2, \tag{28}$$

$$C_o = \langle \psi_c | f_{Co} | \psi_c \rangle = \langle \psi_s | f_{Co} | \psi_s \rangle = \frac{a_o}{k} \Omega, \tag{29}$$

with $a_o = -4ik_{10}^2 / ((\gamma_{10}^2 - 1)c_o)$,

$$\begin{aligned} C_e = \langle \psi_c | f_{Ce} + f_{nh} | \psi_c \rangle &= \langle \psi_s | f_{Ce} + f_{nh} | \psi_s \rangle \\ &= \left(\frac{a_e}{k^2} + b_e \right) \Omega^2, \end{aligned} \tag{30}$$

with

$$\begin{aligned} a_e &= \frac{\gamma_{10}^2 k_{10}^2}{(\gamma_{10}^2 - 1)c_o^2} \left[\zeta + \frac{2i}{\gamma_{10}^2 k_v R} \right], \\ b_e &= \frac{\gamma_{10}^2}{(\gamma_{10}^2 - 1)c_o^2} \left[(\zeta - 1)\gamma - 2i \left(\frac{\gamma - 1}{k_h R} + \frac{1}{\gamma_{10}^2 k_v R} \right) \right], \end{aligned}$$

$$\zeta = 1 - \frac{2}{\gamma_{10}} \frac{J_0(\gamma_{10})}{J_1(\gamma_{10})} + \frac{J_0^2(\gamma_{10})}{J_1^2(\gamma_{10})} \approx 0.7.$$

Then, due to the orthogonality property of the eigenfunctions ψ_s and ψ_c , equation (22b) leads to the following set of linear equations satisfied by the amplitudes A_c and A_s :

$$\begin{pmatrix} D - C_e & C_o \\ -C_o & D - C_e \end{pmatrix} \begin{pmatrix} A_c \\ A_s \end{pmatrix} = \begin{pmatrix} S \\ 0 \end{pmatrix}. \tag{31}$$

In this system of linear equations, the right hand side represents the source of energy (acting only on the mode ψ_1^c), the factor C_o represents the Coriolis cross coupling between the modes labeled ‘‘c’’ ($\cos \varphi$) and ‘‘s’’ ($\sin \varphi$) proportional to the rotation rate Ω , and the factor C_e represents the ‘‘self-coupling’’ of each mode due to both centripetal effects described in equation (15) by the sum $F_{Ce} + F_{nh}$ (in this sum each term is of the same order of magnitude and proportional to the square of the rotation rate). Note that the result emphasized unsurprisingly a behavior analog to a two degrees of freedom oscillator. As expected, the centripetal effects act only on the amplitude and the phase of each mode, like the usual factor D (linked to the dissipation process which occurs essentially in the boundary layers).

The couple of equations (31) can also be obtained in the following manner. Writing the Coriolis terms $\langle G|F_{Co} \rangle = \langle G|f_{Co} |p \rangle$ as an operator $(1 - C_e/D)O = \langle G|f_{Co} \partial_\varphi |$ acting on the unknown acoustic pressure p , and taking into account equations (24), (25) and (27), equation (22b) leads to the following expression:

$$p = p_0 + Op, \tag{32}$$

where $p_0 = S/D/(1 - C_e/D)\psi_c$ represents the pressure variation created by the acoustic source when neglecting the Coriolis coupling in the rotating cavity.

Because the operator O is proportional to the rotation rate Ω , the Born approximation, that is $p_0 + Op \approx (1 + O)p_0$, could be sufficient for the lower rotation rates. But for higher rotation rates, a Dyson series must take place:

$$p_0 + Op = (1 + O + O^2 + O^3 + \dots)p_0. \tag{33}$$

A straightforward analysis lying on the same kind of calculation than the preceding one (equations 25 to 30) gives, thanks to the orthogonality properties,

$$\begin{aligned} p &= \frac{S}{D - C_e} \sum_{n=0}^{\infty} \left(\frac{-C_o^2}{(D - C_e)^2} \right)^n \\ &\quad \cdot \left(\psi_c + \frac{C_o}{D - C_e} \psi_s \right), \end{aligned} \tag{34}$$

that is

$$\begin{aligned} p &= \frac{S}{D - C_e} \frac{1}{1 + C_o^2/(D - C_e)^2} \\ &\quad \cdot \left(\psi_c + \frac{C_o}{D - C_e} \psi_s \right), \end{aligned}$$

which gives the same results as the solution of equation (31) for the amplitudes A_c and A_s , namely

$$A_c = \frac{(D - C_e)S}{(D - C_e)^2 + c_o^2}$$

and

$$A_s = \frac{C_o S}{(D - C_e)^2 + c_o^2}. \quad (35)$$

But equation (34) can also be written in the following manner:

$$p = \frac{S}{D - C_e} \left[\psi_c + \frac{C_o}{D - C_e} \psi_s - \left(\frac{C_o}{D - C_e} \right)^2 \psi_c - \left(\frac{C_o}{D - C_e} \right)^3 \psi_s + \left(\frac{C_o}{D - C_e} \right)^4 \psi_c + \left(\frac{C_o}{D - C_e} \right)^5 \psi_s - \dots \right]. \quad (36)$$

This result permits to interpret the phenomena as recurrent coupling: the mode ψ_c gives rise to the mode ψ_s (with the relative amplitude $C_o/(D - C_e)$) due to the Coriolis coupling, which in turn creates by Coriolis coupling a modal component ψ_c with the relative amplitude $-C_o^2/(D - C_e)^2$ so that the global amplitude of the mode ψ_c changes, and so on. This is the Coriolis “cross-coupling” mentioned above. Close to the resonant frequency (when $|D - C_e|$ is minimum), the amplitudes are opposite in sign alternatively: therefore these resonances are lowered, and are even converted into minimum for higher rotation rates Ω , as shown in the next section (the system acts as a two degrees of freedom oscillating mechanism).

Finally the transfer function of interest (the sensitivity of the rate gyro) is given by

$$\frac{A_s}{A_c} = \frac{C_o}{D - C_e}. \quad (37)$$

This result emphasizes that the sensitivity is proportional to $(D - C_e)^{-1}$ which is proportional to the quality factor when the working frequency is the resonant frequency (defined for the lower rotation rates). For any rotation rate (i.e. from 10^{-2} °/s up to 10^5 °/s) and for a working frequency equal to the frequency of the central extremum amplitude (the maximum for lower rotation rates and the minimum for upper ones), the sensitivity is proportional to the factor C_o , that is proportional to the rotation rate Ω , because the imaginary part of the factor C_e (proportional to Ω^2) is always much lower than the imaginary part of the factor D . Then, tuning the frequency at this extremum of the mode “c” (with an appropriate phase loop), the sensitivity of the acoustic gyro is maximum and its response is linear for any rotation rate accessible above its threshold.

Note that for the lower rotation rates (up to roughly 10^3 °/s) the results (35) and (37) give the approximate results obtained previously [2]:

$$A_c \approx S/D, \quad A_s \approx C_o S/D, \quad \text{and} \quad A_s/A_c \approx C_o/D. \quad (38)$$

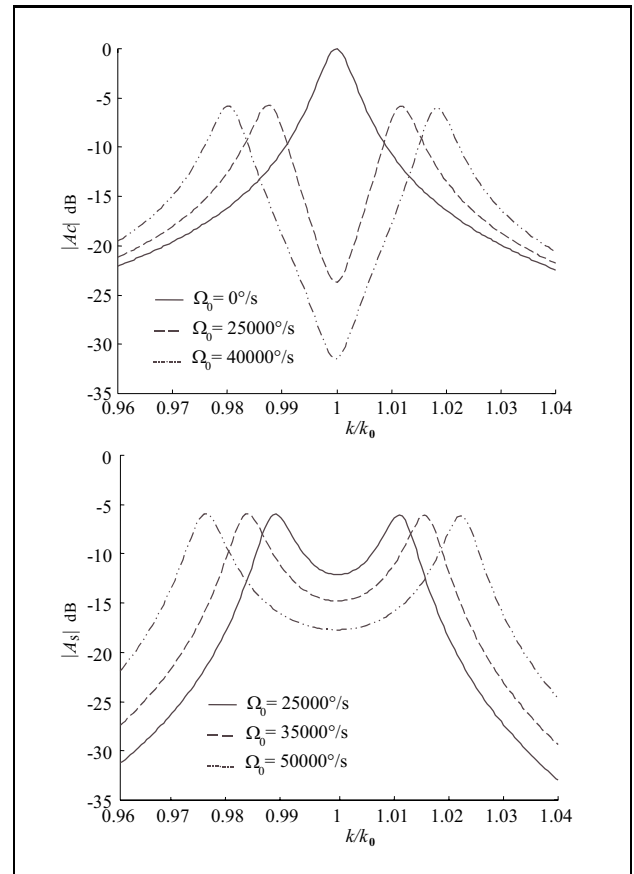


Figure 2. Normalized amplitudes $|A_c(\Omega_0, k)|$ of the mode “c” and $|A_s(\Omega_0, k)|$ of the mode “s” (dB re $|A_c(0, k_0)|$), as functions of the normalised wavenumber k/k_0 , for several rotation rates given on the diagram (theoretical curves).

3.2. Results and conclusion

The theoretical and experimental results given in this section correspond to a cylindrical cavity 4 centimeters in diameter and 1 centimeter high, filled with air at atmospheric pressure $P_0 = 10^5$ Pa and temperature $T_0 = 300$ K. The theoretical results are obtained using the following air constants: $\rho_0 = 1.2$ kg/m³, $C_p = 29.1$ J mol⁻¹ K⁻¹, $\gamma = 1.4$, $\nu = 1.5 \cdot 10^{-5}$ m⁻⁵ m²/s, $\lambda = 25 \cdot 10^{-3}$ W/m/K and $c_0 = 342$ m/s.

For uniform, steady, and lower angular velocities Ω_0 (typically less than 10^3 °/s), the variations of the amplitudes $|A_c|$ of the mode “c” and those of the amplitude $|A_s|$ of the mode “s”, as functions of the angular frequency ($k c_0$), show a resonance [2] (first azimuthal resonance of the cavity) corresponding respectively to the minimum of the absolute value of the factor D in equation (38) given by the value k_0 of k (see curve $\Omega_0 = 0$ °/s in Figure 2 as an example). But, for the uniform, steady, and higher angular velocities Ω_0 (typically greater than 10^3 °/s, up to 10^5 °/s), this resonance is split into two maximums, at frequencies given by the root of the determinant of the square matrix on the left hand side of equation (31), approximately equal to

$$k_{\pm}^2 \approx k_{10}^2 \pm (i a_0 / k_{10}) \Omega_0,$$

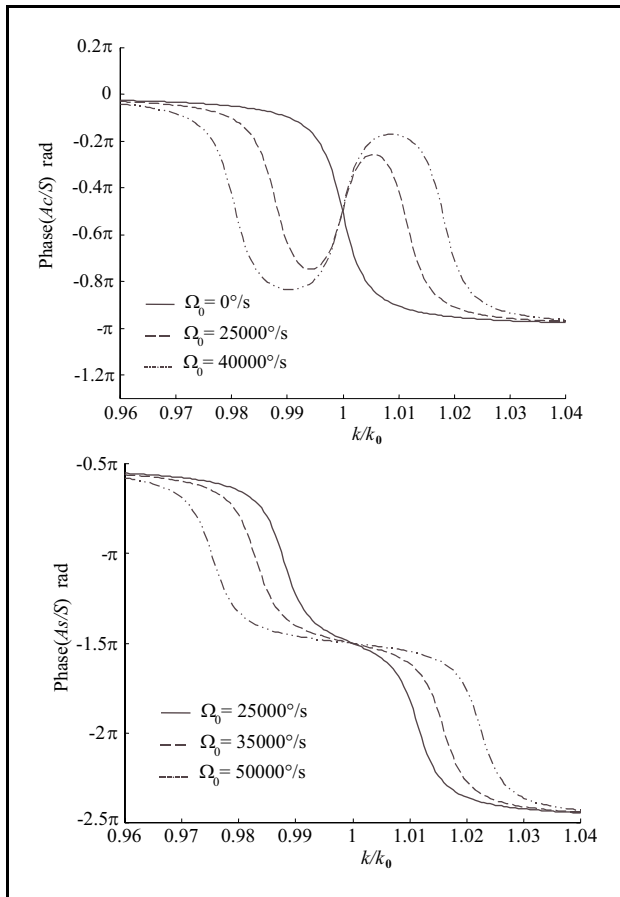


Figure 3. Phases (rad) of A_c/S and of A_s/S , as function of the normalised wavenumber k/k_0 , for several rotation rates given on the diagram (theoretical curves).

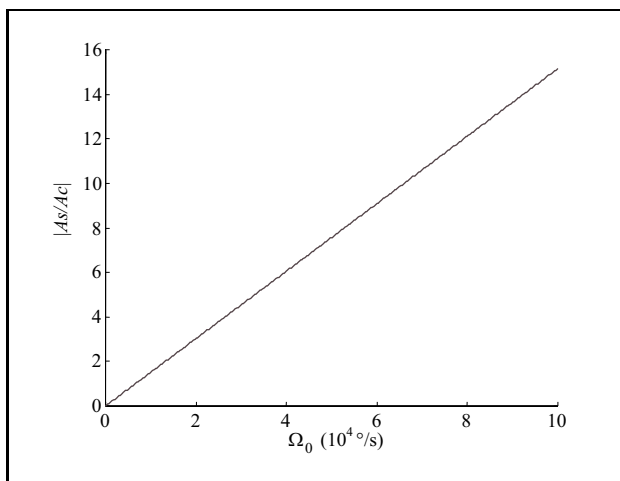


Figure 4. Amplitude of the theoretical transfer function $|A_s/A_c|$ (the normalised response of the rate gyro at the location of the measurement microphone) as function of the rotation rates for the normalised wave number $k/k_0 = 1$.

a minimum occurs for the mode “c” near the central frequency $k = k_0$ (the root of the absolute value of the factor $(D - C_e)$ in equation 35) which depends slightly on the rotation rate (less than 0.04%). The process involved in

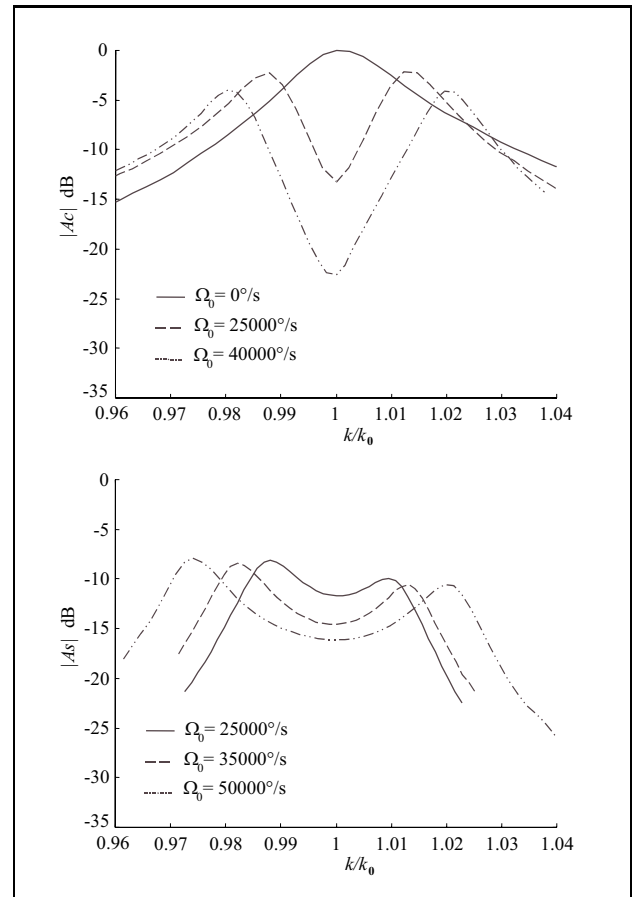


Figure 5. Normalised amplitudes $|A_c(\Omega_0, k)|$ of the mode “c” and $|A_s(\Omega_0, k)|$ of the mode “s” (dB re $|A_c(0, k_0)|$), as functions of the normalised wavenumber k/k_0 , for several rotation rates given on the diagram (experimental curves).

this phenomena is emphasized by the solution (36) of the problem which can be interpreted as follows (as already mentioned above): the Coriolis coupling acts as an energy transfer from the mode “c” ($\cos \varphi$) created by the loud-speaker to the orthogonal mode “s” ($\sin \varphi$), and then, due to the same process, an energy transfer from this mode “s” to the mode “c” occurs but out of phase with respect to the preceding one (close to the resonant frequency), and so on. Therefore, due to these opposite signs, the resonance of each mode (“c” and “s”) is converted into a minimum. The theoretical curves $|A_c|$ and $|A_s|$ (logarithmic scales) versus the normalized wavenumber (k/k_0) shown in Figure 2 are examples of splits of the resonance when the rotation rate Ω increases. The theoretical related phases for A_c and A_s versus k/k_0 are shown in Figure 3 (the reference is the phase of the source term S). At the resonance, these complex amplitudes A_c and A_s are out of phase.

Moreover, if the frequency of the acoustic pressure is tuned in order to be equal to the frequency of the central extremum (maximum for the lower rotation rates and minimum for the higher ones, i.e. $k/k_0 = 1$), the ratio A_s/A_c (equation 37) is proportional to the rotation rate Ω_0 , for any value from the threshold of measurement (10^2 °/s) up to the highest rotation rate accessible (10^5 °/s),

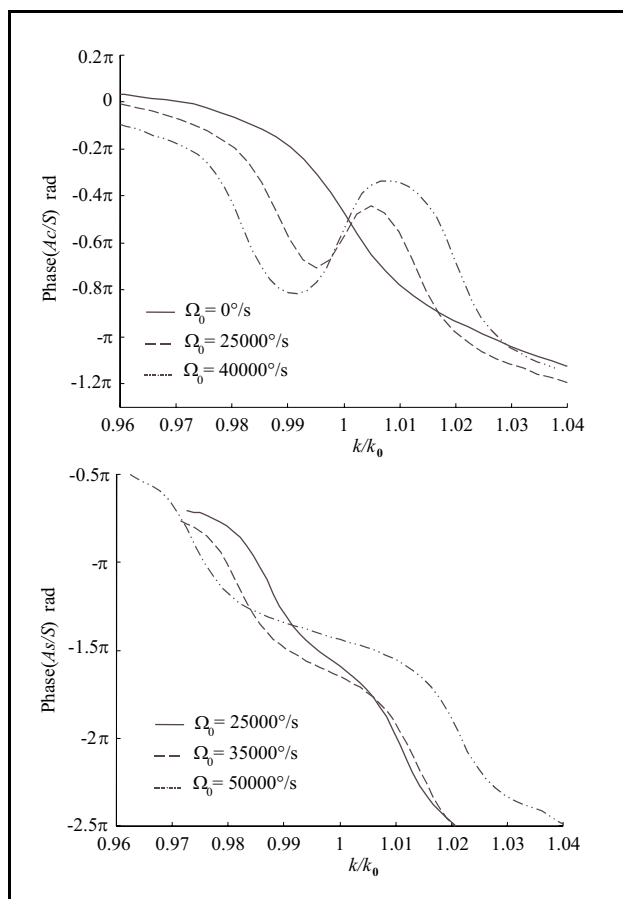


Figure 6. Phases (rad) of A_c/S and of A_s/S , as function of the normalised wavenumber k/k_0 , for several rotation rates given on the diagram (experimental curves).

as shown in Figure 4. The unique (high coast) experiment made in using the high-speed rotating table in Laboratoire de Recherches Balistiques et Aérodynamiques (L.R.B.A.) Vernon, gives evidence of the accuracy of the model in several respects, as mentioned hereafter ; but the electronic device designed for the experiment did not permit to tune the frequency at the central extremum, then did not permit to confirm experimentally this result up to 10^5 °/s.

The experimental results shown in Figure 5 and Figure 6, respectively amplitudes and phases of A_c/S and A_s/S , present the same behaviour than the theoretical one in Figure 2 and Figure 3, revealing however some discrepancies whose the origin is difficult to explain at these very high rotation rates with the device and apparatus used for the measurement.

Nevertheless, it can be emphasised that the experimental results have provide confirmation of the theoretical predic-

tions in having shown the splitting of the maximum (resonance) into three extremums when a high rotation rate occurs, that is when the acoustic modes ($\cos \varphi$) and ($\sin \varphi$) are strongly coupled together (reacting strongly one upon the other). Given the difficulties of the experiences, there is seen to be quite close agreement between these analytical and experimental results, thereby supporting the fact that the acoustic gyro would be a good candidate to measure linearly rotation rates from the threshold [1, 2] 10^{-2} °/s up to the highest rotation rates attainable 10^5 °/s (that is 10^7 times the threshold), the transient response [4] being less than 50 ms. Then this new sensor would be useful in several applications, especially those which require miniaturisation capability, lower manufacturing coast and lower power consumption, as well as higher reliability and improved lifetime.

Acknowledgement

This work has been founded by the Délégation Générale de l'Armement which has supported the research studentship of the first author preparing his thesis that in part led to this paper. The authors are indebted to Guy Tournois, Ing., for the design of the specific electronic circuits needed in the experiments with rotating tables.

References

- [1] M. Bruneau, C. Garing, H. Leblond: A rate gyro based on acoustic mode coupling. *J. Acoust. Soc. Am.* **80** (1986) 672–680.
- [2] P. Herzog, M. Bruneau: Shape perturbation and inertial mode coupling in cavities. *J. Acoust. Soc. Am.* **86** (1989) 2377–2384.
- [3] P. Dupire, M. Bruneau: Transient behavior of acoustic gyrometers. *J. Sound Vib.* **212** (1998) 37–59.
- [4] D. Ecotière, M. Bruneau, N. Tahani: Inertial- and flow-induced acoustic modes coupling in unsteady-rotating cylindrical fluid-filled cavities. *J. Sound Vib.* **252** (2002) 37–63.
- [5] M. Bruneau, A.-M. Bruneau, P. Dupire: A model for rectangular miniaturized microphones. *Acta Acustica* **3** (1995) 275–282.
- [6] P. Hamery, P. Dupire, M. Bruneau: Acoustic fields in trapezoidal cavities. *Acustica/Acta Acustica* **83** (1997) 13–18.
- [7] T. Bourouina, A. Exertier, S. Spirkovitch: Preliminary results on a silicon gyrometer based on acoustic mode coupling in small cavities. *J. Microelectromechanical Systems* **4** (1995) 347–354.
- [8] A. D. Pierce: *Acoustics*, 2nd edition. American Institute of Physics, Woodbury, NY, 1989.
- [9] M. Bruneau: *Manuel d'acoustique fondamentale*. Hermès, Paris, 1998.